Received: 29 August 2019 | Accepted: 13 January 2020

DOI: 10.1002/jcp.29570

Journal of Cellular Physiology WILEY

ORIGINAL RESEARCH ARTICLE

MicroRNA-206 upregulation relieves circTCF25-induced osteosarcoma cell proliferation and migration

Yongkun Wang[1] | Shaomin Shi[2] | Qiao Zhang[1] | Hang Dong[1] | Jingzhe Zhang[1]

[1]Department of Orthopaedics, China-Japan Union Hospital of Jilin University, Changchun, Jilin, China

[2]Department of Respiratory, China-Japan Union Hospital of Jilin University, Changchun, Jilin, China

Correspondence
Jingzhe Zhang, Department of Orthopaedics, China-Japan Union Hospital of Jilin University, 126 Xiantai Street, Changchun, 130033 Jilin, China.
Email: zhangjz0042@sina.com

Abstract

Circular RNA TCF25 (circTCF25) has been proven to be upregulated in human malignancy and correlated with tumor process. Our study aimed to unravel whether circTCF25 dictates cellular activities of osteosarcoma cells and address the possible mechanisms associated with microRNA (miR). circTCF25 and miR-206 in clinical specimens from 25 patients suffering from osteosarcoma were quantified by quantitative reverse transcription-polymerase chain reaction (qRT-PCR). circTCF25- or miR-206-overexpressed cells (MG-63 and Saos-2) were constructed by transfection and confirmed by qRT-PCR, and continually subjected to cascades of assays for viability by Cell Counting Kit-8, proliferation by $BrdU^+$, migration, and invasion by Transwell chamber and proteins involved in proliferation (cyclin D1 and CDK6), migration and invasion (MMPs, TIMP-1, and vimentin) and signaling transduction (mitogen-activated protein kinase [MEK], extracellular signal-regulated kinase [ERK], protein kinase B [AKT], mammalian target of rapamycin [mTOR]) by western blot. Targeting the relationship between miR-206 and circTCF25 was validated by the Dual-Luciferase Reporter System. circTCF25 was apparently enriched while miR-206 was deficient in osteosarcoma specimens. circTCF25 elevated viability, facilitated proliferation, and fortified migration and invasion capacities of MG-63 and Saos-2 cells. Besides, miR-206 was downregulated in circTCF25-replenished cells. However, miR-206 upregulation offset the carcinogenesis of circTCF25. miR-206 had the ability to downregulate circTCF25 by targeting it. Of note, circTCF25 drove the phosphorylation of signaling transducers while miR-206 upregulation relived the effect of circTCF25 on the phosphorylation. circTCF25 conferred carcinogenesis in osteosarcoma cells through and suppressing miR-206 expression. However, miR-206 overexpression buffered the carcinogenesis of circTCF25.

KEYWORDS

AKT/mTOR, circTCF25, MEK/ERK, microRNA-206, osteosarcoma

1 | INTRODUCTION

Osteosarcoma is the most usual primary malignant bone tumor and typically happens among children, adolescence, and young adults (Misaghi, Goldin, Awad, & Kulidjian, 2018). The disease has a strong potential in invasion and distant metastasis which is responsible for high lethality (Smeland et al., 2019). During the last 30 years, advancement in management strategy, including neoadjuvant chemotherapy, surgical removal of primary tumors and evident metastatic tissues, and adjuvant chemotherapy after surgery, has improved prognosis (Isakoff, Bielack, Meltzer, & Gorlick, 2015). On the basis of the bioinformatics analysis, a large scale of noncoding RNA, containing circular RNAs (circRNAs), long

noncoding RNAs (lncRNAs), and microRNAs (miRNAs), is possibly implicated in exploration of underlying mechanisms associated with biological processes (Ali, Hu, Qian, Chen, & Yang, 2018; Palmini, Marini, & Brandi, 2017; C. Wang, Ren, Zhao, Wang, & Wang, 2018), which implies that these small molecules might be helpful for the diagnosis and improvement of the efficacy of therapeutic treatment of osteosarcoma.

Hundreds of circRNAs have been discovered to be dysregulated in distinct cancers, for instance, and it is becoming cumulatively apparent that circRNAs are significant in the pathogenesis of cancer (C. Wang et al., 2018). Bioinformatics analysis has been carried out to reveal the differential expression of circRNA which might indicate the occurrence and advance of osteosarcoma (Xi et al., 2019). Actually, circRNAs are not only steady byproducts of messenger RNA (mRNA) after splicing but rather an outcome of alternative splicing (Dehghannasiri, Szabo, & Salzman, 2019). Said differently, circRNAs per se play a regulatory role in gene expression, which has been confirmed in plenty of studies. To be specific, circRNAs modulate the mRNA level through acting as miRNAs sponge (G. Chen et al., 2018; Li et al., 2019). circTCF25 (circRNA ID: hsa_circ_0041103) has been sustained to be upregulated in bladder carcinoma and its upregulation is responsible for proliferation and migration and invasion (Zhong, Lv, & Chen, 2016). However, it still remains enigmatic whether circTCF25 dictates the growth of osteosarcoma cells.

The dynamics of gene expression are extremely sophisticated in cancer pathology since the biological roles of RNA molecules. For example, miR-206 is known to suppress cell proliferation through directly targeting cyclin in a wide spectrum of malignant tumors (Elliman et al., 2014; L. Zhang et al., 2013; J. Zhou et al., 2013). In osteosarcoma, studies proved that miR-206 is downregulated in osteosarcoma cells and primary tumor specimens, and its underexpression is closely connected with poor histological differentiation, metastasis, T classification, and advanced clinical stage (Bao et al., 2013). Interestingly, miR-206 has been found to be modulated by lncRNAs which function as a competing endogenous RNA, and then mediate tumor growth and metastasis (S. H. Wang et al., 2016). As another noncoding RNA, circRNAs are still unexplored whether they can be in conjunction with miR-206 to participate in regulating the cancer process, not to mention circTCF25.

Altogether, our studies substantiated the biological implications of circTCF25/miR-206 in the development of osteosarcoma, which need to be addressed for the facilitation in the translation of fundamental circRNA research to clinical application.

2 | MATERIALS AND METHODS

2.1 | Clinical specimens

To investigate circTCF25 in osteosarcoma, a total of 50 pairs of osteosarcoma bones and morphologically normal tissues were collected from 50 patients with osteosarcoma who were undergoing surgery at the Department of Orthopaedics at China-Japan Union Hospital of Jilin University (Changchun, China). Tissue specimens were snap-frozen in liquid nitrogen for circTCF25 and miR-206 analysis by qRT-PCR. Our study was performed with permission from the Ethics Committee of China-Japan Union Hospital of Jilin University and was in compliance with the criterion and standard. The pathological characteristics were suggested in Table 1.

TABLE 1 Association of circTCF25 expression with pathological parameters of osteosarcoma bone tissues from 50 patients

Parameters	circTCF25 expression		*p* Value
	Low group	High group	
Gender			
Male	16	17	.934
Female	8	9	
Ages (years)			
<18	13	14	.789
≥18	11	12	
Tumor location			
Femur	14	14	.587
Tibia	6	8	
Humeral bone	4	4	
Histological type			
Osteoblastic	12	14	
Chondroblastic	5	6	.875
Fibroblastic	4	3	
Telangiectatic	3	3	
Tumor grade			
Low	16	7	.029*
High	8	19	
Metastasis			
Positive	8	16	.046*
Negative	16	10	

Note: Significant difference.
Abbreviation: circTCF25, circular RNA TCF25.
*$p < .05$.

2.2 | Cell culture and stimulation

Human osteosarcoma bone cell lines MG-63 (Item no.: CRL-1427) and Saos-2 (HTB-85) were purchased from American Type Culture Collection (ATCC, Rockville, MD). MG-63 cells were cultured in minimum essential medium (Gibco, Gaithersburg, MD) in addition to 10% fetal bovine serum (FBS; Gibco) at 37°C in a humidified condition (95% air and 5% CO_2). Sao-2 cells were incubated in McCoy's 5a Medium (Gibco) supplemented with 15% FBS in an incubator (95% air and 5% CO_2) at 37°C.

2.3 | circTCF25 and miR-206 overexpression

To induce circTCF25 overexpression in MG-63 and Saos-2 cells, pCDH (Ribobio, Guangzhou, China) harboring front and back circular frames of circTCF25 was constructed by Geenseed (Guangzhou, China). Briefly, 10,000 cells were seeded in a well of 24-well plates

and continually incubated with the mix of DNA and Lipofectamine 2000 reagent (1:2.5; Invitrogen, Carlsbad, CA). miR-206 mimic and its counterpart (negative control mimic, NC mimic) was synthesized by GenePharma (Shanghai, China). circTCF25 and miR-206 mimic were simultaneously or separately introduced into MG-63 and Sao-2 cells in the presence of Lipofectamine 2000 reagent. In short, 6,000 cells each well in a 96-well plate were incubated with 3 pmol miRNA-206 mimic in the presence of 1.0 μl of Lipofectamine 2000 reagent. Experiments were performed in triplicate and repeated three times.

2.4 | Cell viability assay

The viability of MG-63 and Saos-2 cells were examined using Cell Counting Kit-8 (CCK-8) solution (APExBIO, Houston, TX) consisting of water-soluble tetrazolium salt, (2-(2-methoxy-4-nitrophenyl)-3-(4-nitrophenyl)-5-(2, 4-disulfophenyl)-2H-tetrazolium,monosodium salt), and electron mediators. In short, MG-63 and Sao-2 cells were preincubated in a 96-well plate for 24 hr in a density of 5,000 cells per well. Next, 10 μl of CCK-8 solution was added into the plate and incubated with the cells for 1 hr. Continually, the absorbance was read at 450 nm using a microplate reader (Molecular Devices, San Jose, CA). Experiments were performed in triplicate and repeated three times.

2.5 | Proliferation assay

A pyrimidine analog, 5-bromo-2-deoxyuridine (BrdU) was used to monitor the proliferative activity of MG-63 and Saos-2 cells since BrdU can get incorporated into the newly generated DNA in lieu of thymidine. BrdU cell proliferation assay kit was used (BioVision, Milpitas, CA). In short, MG-63 and Saos-2 cells were plated on a 96-well plate in a density of 5,000 cells each well and incubated for 24 hr. Next, BrdU solution was added into each well according to the user's manual and incubated with the cells for 1 hr at 37°C. The medium was removed and 100 μl of the fixing-denaturing solution was added into each well, followed by incubated for 30 min at room temperature. The culture was supplemented with BrdU detection antibody and incubated for 1 hr at room temperature. After washed in wash buffer, the BrdU detection antibody was hybridized using horseradish peroxidase (HRP)-linked antibody for 1 hr at room temperature. Finally, 100 μl of TMB substrate was added into each well, and the final incubation was carried out for 5 min. After 100 μl of stop solution was added, the absorbance was read at a wavelength of 450 nm using a microplate reader. Experiments were performed in triplicate and repeated three times.

2.6 | Migration and invasion

To investigate migration and invasion capacities of MG-63 and Saos-2 cells, Transwell chambers coated with or without Matrigel matrix (BD Biosciences, Franklin Lakes, NJ) was applied. To examine invasion behavior, the cells in FBS-free media were grown on the Matrigel-coated membrane of 24-well culture plates and incubated for 24 hr. The lower chamber was supplemented with culture media containing 10% FBS. Noninvasive cells were wiped out using a cotton swab, and invasive cells were stained by 0.1% crystal violet (Sigma-Aldrich, St. Louis, MO) and counted. Experiments were performed in triplicate and repeated three times. Experiments were performed in triplicate and repeated three times.

2.7 | Luciferase reporter assay

psiCheck plasmid (Promega, Madison, WI) harboring the sequence coding circTCF25 functioned as a wild-type of circTCF25 (circTCF25-WT). To construct the mutant type (circTCF25-MUT), in-fusion cloning kit (Clontech, Mountain View, CA) was applied in accordance with the product instruction. To validate the targeting relationship, 293T/17 cells (ATCC) were transfected with NC mimic or miR-206 mimic and circTCF25-WT and circTCF25-MUT using Lipofectamine 2000. The fluorescence was generated using the Dual-Luciferase Reporter Assay System (Promega), and was detected by Turner Biosystems (Promega). pRL-TK (Promega) was applied for correcting the diversity.

2.8 | Quantitative reverse transcription-polymerase chain reaction

Total RNA was collected from tissues and cells using TRIzol RNA extraction kit (Invitrogen) according to the manufacturer's protocol. To quantify miR-206, the reverse reaction was performed using RNA extract as a template using the TaqMan miRNA Reverse Transcription kit (Applied Biosystems, Foster City, CA). Then polymerase chain reaction (PCR) was carried out using miR-206 TaqMan microRNA assay (Thermo Fisher Scientific, Waltham, MA) and the specific primers (forward 5′-CCCAACAAGCTCTGCCTG-3′ and reverse 5′-GGGAG CATAGTTGACCTGAAAC-3′) according to the manufacturer's instructions. U6 was used as an internal reference to normalize miR-206 expression with the comparative cycle threshold method ($2^{-\Delta\Delta C_t}$ method). To quantify circTCF25, RNA extract was incubated with RNase R (Epicenter, Madison, WI) for deleting linear RNA. Then complementary DNA (cDNA) was synthesized using Superscript VILO cDNA Synthesis Kit (Thermo Fisher Scientific). PCR was carried out using SYBR Green I Master Kit (Thermo Fisher Scientific) and the specific divergent primers (forward 5′-CACTGGCGTATTTCCTGCTG-3′ and reverse 5′-ATCTGCTTGTAGAGGGCCAG-3′). The expression of circTCF25 was calculated using $2^{-\Delta\Delta C_t}$ method and normalized to GAPDH. Experiments were performed in triplicate and repeated three times.

2.9 | Western blot assay

Total proteins from the clinical tissues and cells were lysed using precold radioimmunoprecipitation assay buffer (Beyotime,

Shanghai, China) in addition with protease inhibitors (Thermo Fisher Scientific). Protein content was examined using bicinchoninic acid assay protein assay kit from Pierce (Appleton, WI). After electrophoresis, the separated proteins were transferred onto polyvinylidene difluoride membranes. Then the membranes were sealed using 5% fat-free milk in TBS-T, followed by incubated with primary antibodies against interest proteins, including cyclin D1 (1:200; ab16663; Abcam, Cambridge, UK), CDK6 (1:1,000, ab151247; Abcam), β-actin (1:1,000, 4967; CST, Danvers, MA), MMP-2 (1:1,000, 87809; CST), MMP-9 (1:1,000, ab38898; Abcam), TIMP-1 (1:1,000, ab61224; Abcam), vimentin (1:1,000, ab137321; Abcam), MEK1/2 (1:1,000, 9126; CST), phospho-MEK1/2 (Ser217/221) (1:1,000, 9154; CST), ERK1/2 (1:1,000, 9102; CST), phospho-ERK1/2 (Thr202/Tyr204) (1:1,000, 4370; CST), AKT (1:1,000, 9272; CST), phospho-AKT (Ser473) (1:2,000, 4060; CST), mTOR (1:1,000, 2972; CST), phospho-mTOR (Ser2481) (1:1,000, 2974; CST) at 4°C overnight. Protein signals were detected using a HRP-conjugated secondary antibody (1:5,000, ab6721; Abcam) and Immobilon Western Chemiluminescent HRP substrate (Millipore, Bedford, MA). Bio-Rad ChemiDoc XRS system (Bio-Rad, Hercules, CA) was used to capture the protein signals and signal intensity was digitized using Image Lab software (Bio-Rad). Experiments were performed in triplicate and repeated three times.

2.10 | Statistical analysis

Data were depicted as the mean ± standard deviation. Statistical analysis was performed with the GraphPad Prism software from GraphPad (San Diego, CA). Student's *t*-test or one-way analysis of variance followed by Bonferroni's test was exploited to compare the differences. *p* value less than .05 was considered to present the statistical difference.

3 | RESULTS

3.1 | circTCF25 was highly expressed in osteosarcoma tissues and elevated cell viability, proliferative activities

The expression of circTCF25 in the osteosarcoma bone tissues was upregulated and evidently higher in comparison with their adjacent tissues (Figure 1a; $p < .001$). The pathological parameters were suggested in Table 1. Notably, a tumor with a high grade showed an accumulation of circTCF25, suggesting the association of circTCF25 expression with the tumor grade ($p < .05$). In addition, high levels of circTCF25 were detected in tumors with a metastatic characteristic ($p < .05$). To further evaluate the role of circTCF25 in

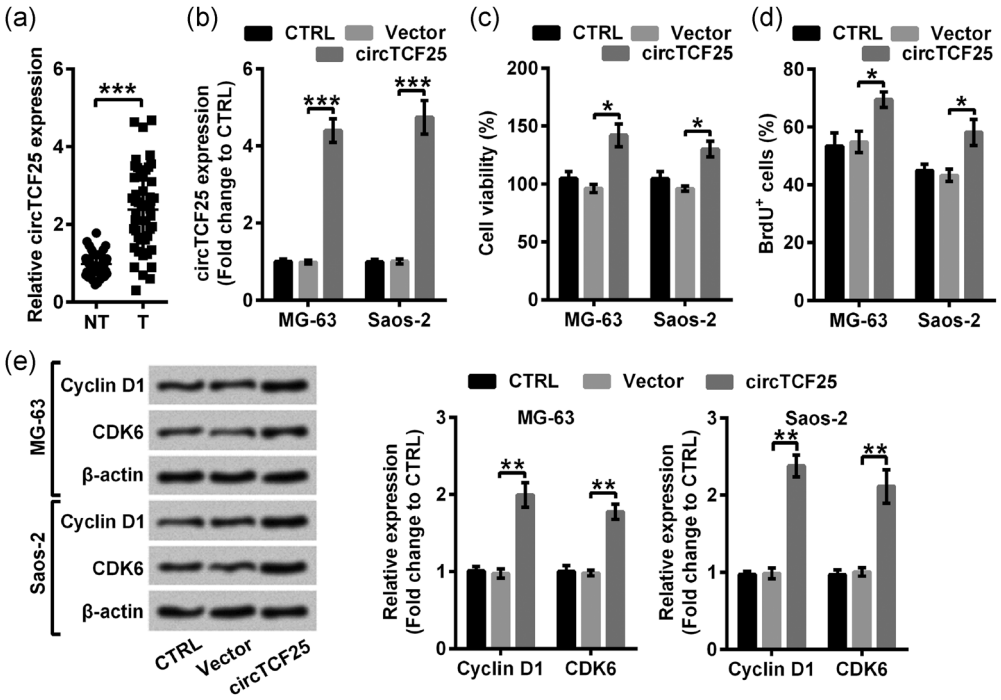

FIGURE 1 circTCF25 was enriched in osteosarcoma bone tissues and increased cell viability and proliferation in MG-63 and Saos-2 cells. (a) High levels of circTCF25 were quantified by qRT-PCR in osteosarcoma bone tissues. T and NT stood for tumor and nontumor specimens, respectively, from 50 patients with osteosarcoma. MG-63 and Saos-2 cells were transfected with plasmids harboring circTCF25, and after transfection (b) circTCF25 level was examined by qRT-PCR, (c) cell viability by Cell Counting Kit-8 reagent, (d) proliferation by BrdU kit, and (e) interest proteins involved in proliferation by western blot assay. Quantitative results of qRT-PCR and western blot were presented as relative expression. The data were representative of average from three independent experiments. BrdU, 5-bromo-2-deoxyuridine; circTCF25, circular RNA TCF25; CTRL, control; qRT-PCR, quantitative reverse transcription-polymerase chain reaction. *$p < .05$, **$p < .01$, ***$p < .001$ presented a significant difference

osteosarcoma, MG-63 and Saos-2 cells were transfected with pCDH harboring circTCF25 and empty vector, which suggested high transfection efficiency (Figure 1b; both $p < .001$). Results from CCK-8 assay suggested that the viability of MG-63 and Saos-2 cells were elevated in circTCF25-transfected cells compared with the cells transfected with empty vector (Figure 1c; both $p < .05$). Consistently, circTCF25-transfected cells showed an increase in proliferative activity (Figure 1d; both $p < .05$). Moreover, circTCF25 resulted in an apparent accumulation of cyclin D1 and CDK6 (Figure 1e; both $p < .01$). Collectively, circTCF25 increased the viability and facilitated the proliferation of osteosarcoma bone cells.

3.2 | circTCF25-induced migration and invasion of osteosarcoma bone cells

To confirm the effects of circTCF25 on the migration and invasion capacities in vitro, a Transwell chamber assay was performed. The cells transfected with circTCF25 exhibited notable inclines in migration and invasion activities compared with the cells transfected with an empty vector (Figure 2a,b; both $p < .05$). Furthermore, circTCF25 overexpression induced the accumulation of MMP-2 and MMP-9 (Figure 2c; both $p < .01$). Conversely, circTCF25 governed the abundance of TIMP-1 (Figure 2c; both $p < .05$). As for vimentin, its expression was upregulated in transfectants (Figure 2c; both $p < .001$). Consequently, circTCF25 overexpression induced migration and invasion behaviors of osteosarcoma bone cells.

3.3 | circTCF25 promoted the growth of osteosarcoma bone cells upon the premise that miR-206 was downregulated

To determine the level of miR-206 in osteosarcoma tissues, qRT-PCR was implemented. As shown in Figure 3a, miR-206 was significantly downregulated in tumor tissues ($p < .05$). Through qRT-PCR analysis, we found circTCF25-transfected MG-63 and Saos-2 cells showed a decrease in miR-206 expression (Figure 3b; both $p < .01$). To assess the role of miR-206, MG-63 and Saos-2

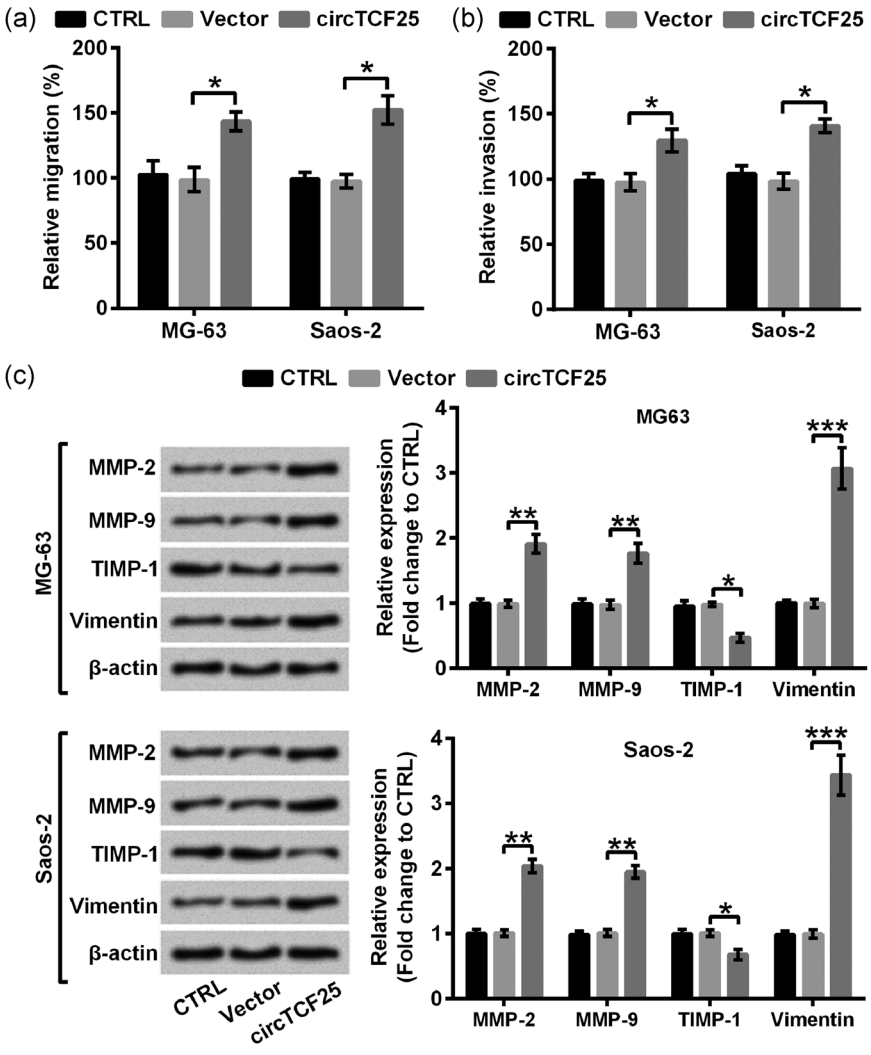

FIGURE 2 Transfection of circTCF25 facilitated migration and invasion of osteosarcoma bone cell lines MG-63 and Saos-2. After transfection, (a) migration and (b) invasion were examined by the Transwell chamber assay kit as described in Section 2. (c) Interest proteins associated with metastasis ability were determined by western blot assay. Protein bands were representative of one of three independent experiments, and the bar graph depicted the signal intensity that reflected the protein level. The data were representative of average from three independent experiments. circTCF25, circular RNA TCF25; CTRL, control. $^{*}p < .05$, $^{**}p < .01$, $^{***}p < .001$ presented a significant difference

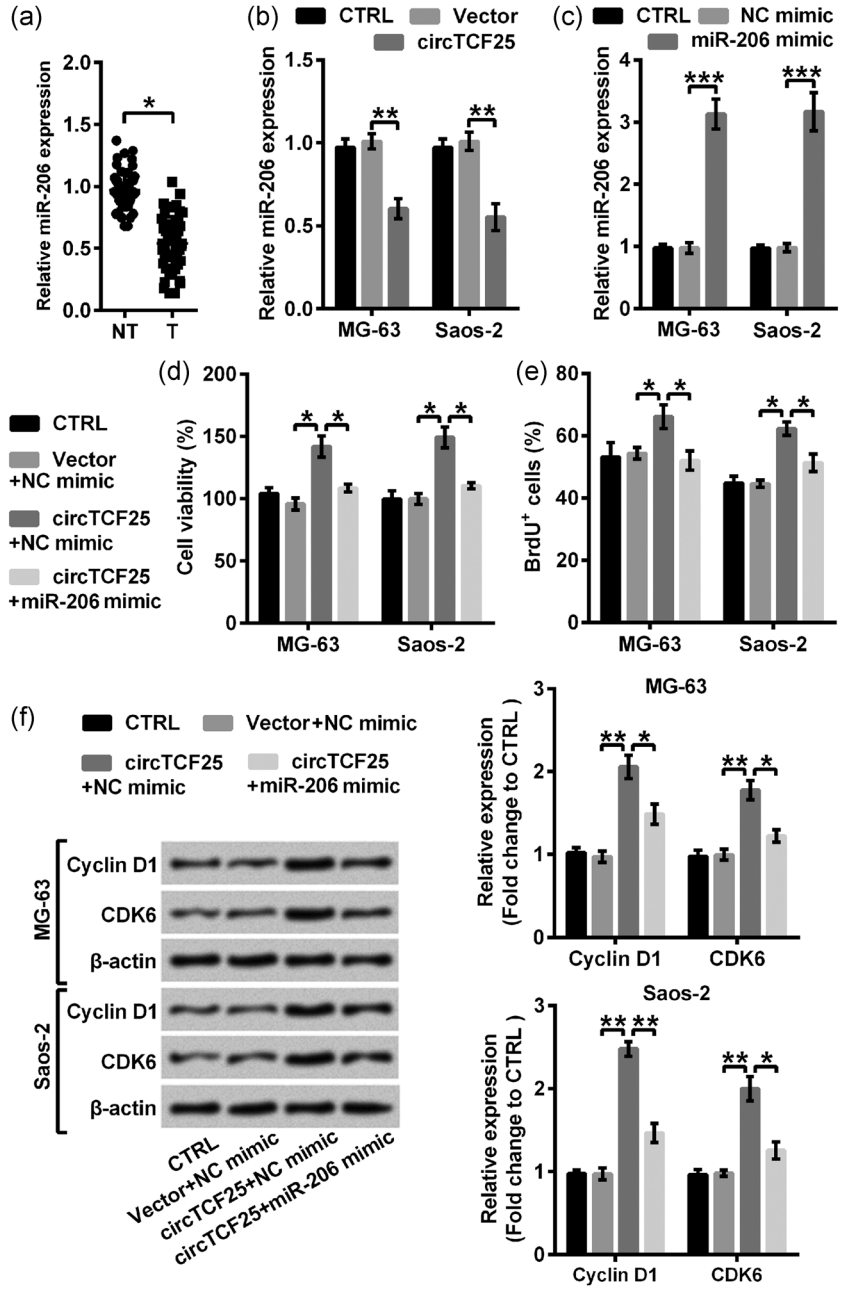

FIGURE 3 miR-206 mimic restrained the effects of circTCF25 overexpression on cell viability and proliferation. (a) Low levels of miR-206 were quantified by qRT-PCR in osteosarcoma bone tissues. (b) The reduction of miR-206 detected by qRT-PCR was observed in circTCF25-replenished MG-63 and Saos-2 cells. MG-63 and Saos-2 cells were introduced with miR-206 mimic, and then (c) miR-206 expression was quantified by qRT-PCR. After simultaneously transfectiond with circTCF25 and miR-206, (d) cell viability by Cell Counting Kit-8 assay kit, (e) proliferation by BrdU incorporation method, and (f) proliferation-related proteins by western blot. Quantitative data of qRT-PCR and western blot were expressed as relative expression. The data were representative of average from three independent experiments. BrdU, 5-bromo-2-deoxyuridine; circTCF25, circular RNA TCF25; CTRL, control; qRT-PCR, quantitative reverse transcription-polymerase chain reaction. $^{*}p < .05$, $^{**}p < .01$, $^{***}p < .001$ presented a significant difference

cells were introduced with miR-206 mimic and NC mimic, and its high expression was depicted in Figure 3c (both $p < .001$). Simultaneous upregulation of circTCF25 and miR-206 caused a significant decrease in viability (Figure 3d; both $p < .05$) and proliferation (Figure 3e; both $p < .05$) compared with single upregulation of circTCF25. Coincidentally, MG-63 and Saos-2 cells enforced to synchronously express circTCF25 and miR-206 showed significant decreases in cyclin D1 (Figure 3f; $p < .05$ or $p < .01$) and CDK6 (Figure 3f; both $p < .05$). Besides, miR-206 mimic impeded migration (Figure 4a; both $p < .05$) and invasion (Figure 4b; both $p < .05$) behaviors induced by circTCF25. Moreover, MMP-2 ($p < .05$ or $p < .01$), MMP-9 (both $p < .05$), and vimentin (both $p < .01$) were repressed by a miR-206 mimic in circTCF25-transfected cells, while TIMP-1 (both $p < .05$) was enhanced (Figure 4c). Then we performed Dual-Luciferase Reporter assay to validate the targeting relationship between miR-206 and circTCF25. Actually, miR-206 repressed the expression of circTCF25 by targeting circTCF25 (Figure 5; $p < .01$). Thus, we concluded that circTCF25 might promote the process of osteosarcoma bone cells through repressing miR-206 expression.

3.4 | circTCF25 triggered signaling transduction of MEK/ERK and AKT/mTOR through repressing miR-206

Western blot assay was carried out to monitor the alteration of signaling transducers in MEK/ERK and AKT/mTOR pathways. circTCF25 upregulation obviously facilitated the phosphorylation of

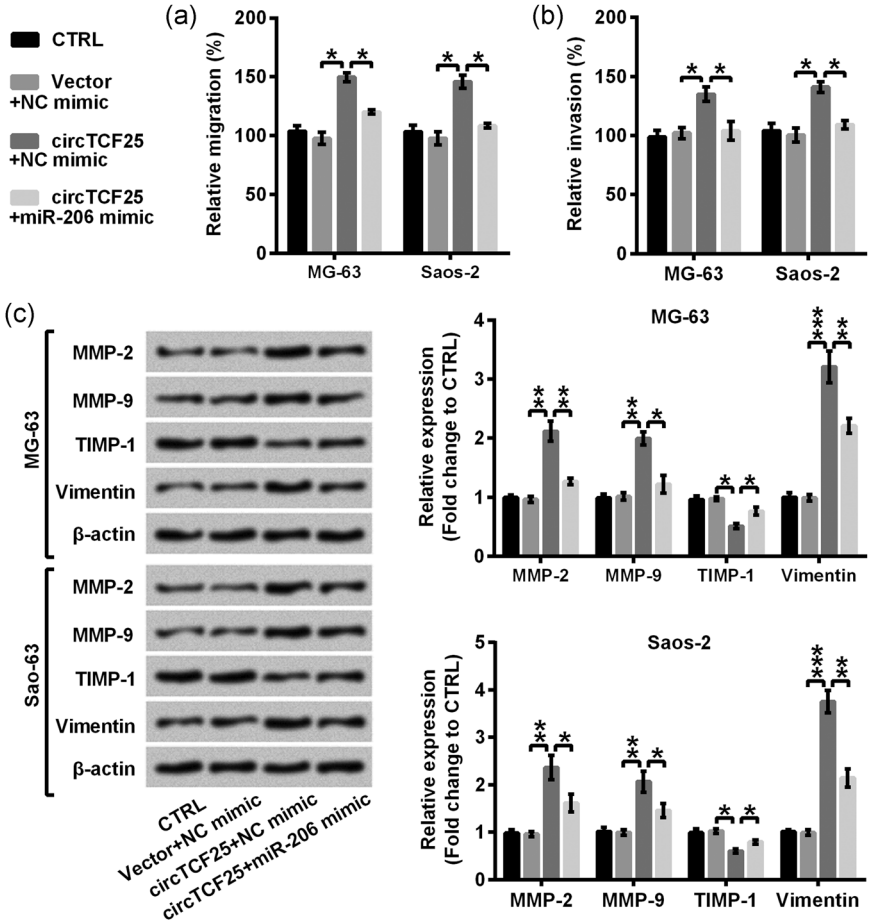

FIGURE 4 circTCF25-induced migration and invasion were blocked by a miR-206 mimic. circTCF25 and miR-206 were concurrently upregulated in MG-63 and Saos-2 cells, and then the cells were subjected to (a) migration and (b) invasion assay using the Transwell chamber kit as described in Section 2. (c) Interest proteins associated with metastasis ability were determined by western blot assay. Protein bands were representative of one of three independent experiments, and the bar graph depicted the signal intensity that reflected the protein level. The data were representative of average from three independent experiments. circTCF25, circular RNA TCF25; CTRL, control. $^{*}p < .05$, $^{**}p < .01$, $^{***}p < .001$ presented a significant difference

MEK ($p < .05$ or $p < .01$), ERK (both $p < .01$; Figure 6a), AKT (both $p < .001$), and mTOR (both $p < .01$; Figure 6b). However, the phosphorylation of MEK (both $p < .05$), ERK (both $p < .05$), AKT (both $p < .01$) and mTOR (both $p < .05$) was suppressed in by miR-206 in circTCF25-downregulated cells (Figure 6a,b). Thus, circTCF25 might induce the activation of signaling transduction, including MEK/ERK and AKT/mTOR via downregulating miR-206.

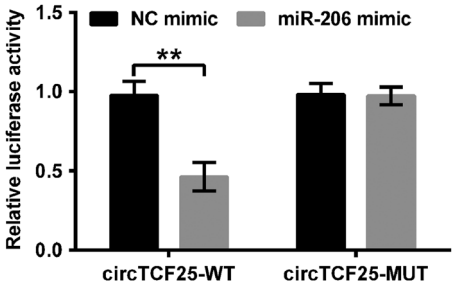

FIGURE 5 circTCF25 was targeted by miR-206. 293T/17 cells were transfected with NC mimic or miR-206 mimic and wild-type-circTCF25 (circTCF25-WT) or mutant type-circTCF25 (circTCF25-MUT). The fluorescence activity was detected using the Dual-Luciferase Reporter Assay System and corrected by pRL-TK. The data were representative of average from three independent experiments. circTCF25, circular RNA TCF25; CTRL, control. $^{**}p < .01$ presented a significant difference

4 | DISCUSSION

In this study, we found the abundance of circTCF25 and deficiency of miR-206 in osteosarcoma bone tissues, and circTCF25 upregulation facilitated the growth of osteosarcoma bone cells by repressing miR-206. Mechanically, circTCF25 might drive signaling transduction of MEK/ERK and AKT/mTOR pathways through suppressing miR-206 in MG-63 and Saos-2 cells. Consequently, we presented that circTCF25 may be applied as a therapeutic target that has a potential in the treatment of osteosarcoma.

Recently, circRNA expression profiles in bladder cancer showed that circTCF25 is significantly upregulated and potentially represents a diagnostic biomarker for bladder cancer (Zhong et al., 2016). Here, we noticed an ectopic expression of circTCF25 in tumor specimens from patients with osteosarcoma. However, not much is known about how the biogenesis is exactly modulated. Considering that circTCF25 mediated the expression of target genes associated with proliferation and migration and invasion (Zhong et al., 2016), we analyzed these likewise. Consistently, circTCF25 facilitated proliferation and migration and invasion. Interestingly, circTCF25 affected the hallmarks of these cellular activities. A pioneer study pointed out that circFoxo3 blocks cell cycle through interacting with p21-CDK2 to constitute a ternary complex (Du et al., 2016). In consistent with our findings, circTCF25 mediates migration and invasion through affecting the expression of MMPs, and vimentin (Luo et al., 2017; Wang & Li, 2018).

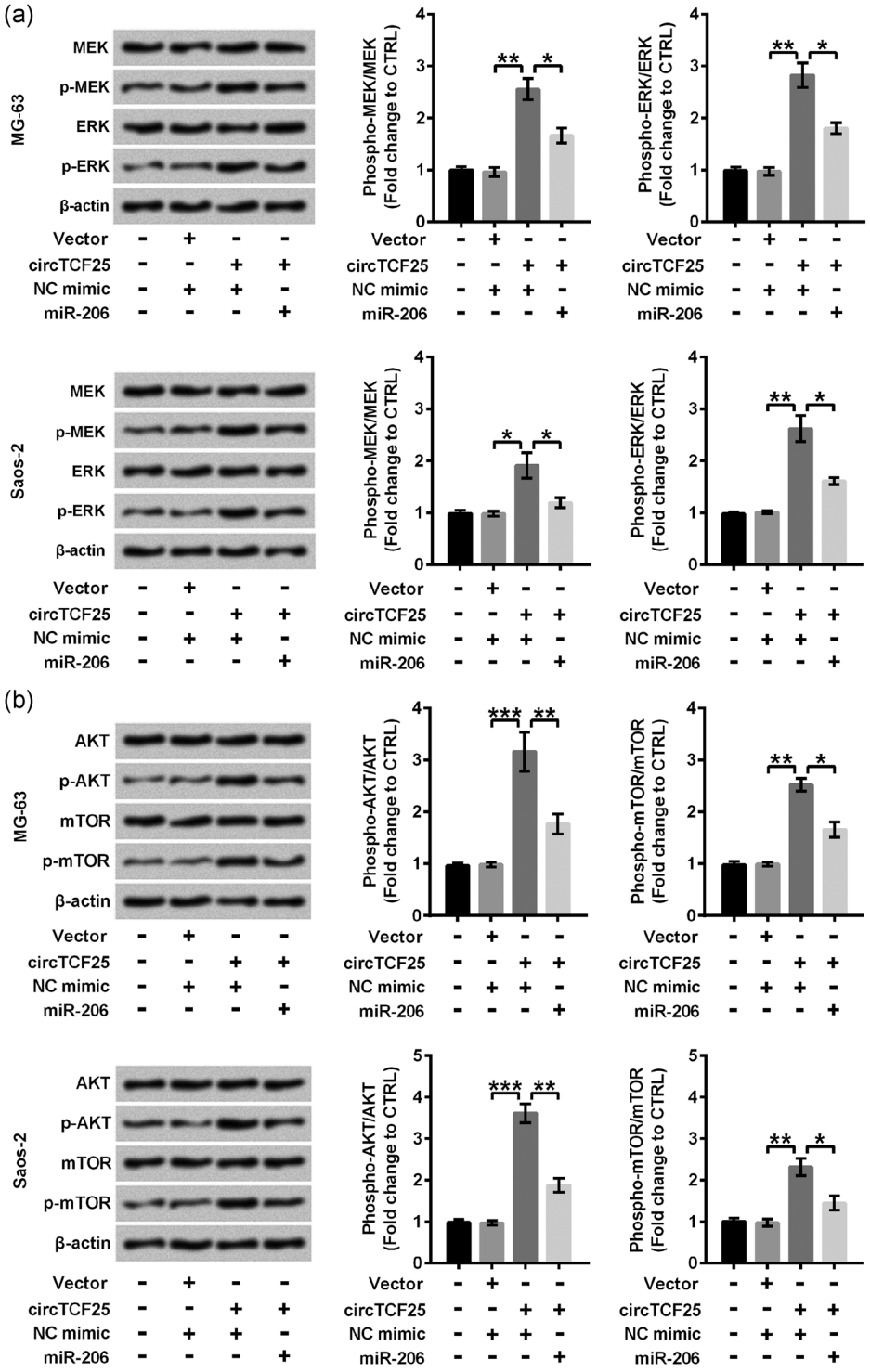

FIGURE 6 miR-206 mimic dampened signaling transduction of MEK/ERK and AKT/mTOR induced by circTCF25 in osteosarcoma bone cells. circTCF25- and miR-206-replenished MG-63 and Saos-2 cells were subjected to western blot assay for signaling transducers, including (a) MEK, phospho-MEK (Ser217/221), ERK, phospho-ERK (Thr202/Tyr204), (b) AKT, phospho-AKT (Ser473), mTOR, and phospho-mTOR (Ser2481). Protein bands were representative of one of three independent experiments, and the bar graph depicted the signal intensity that reflected the protein level. The data were representative of average from three independent experiments. AKT, protein kinase B; circTCF25, circular RNA TCF25; ERK, extracellular signal-regulated kinase; MEK, mitogen-activated protein kinase kinase 1; mTOR, mammalian target of rapamycin. $^{*}p < .05$, $^{**}p < .01$, $^{***}p < .001$ presented a significant difference

Moreover, we found TIMP-1 was downregulated in circTCF25-replenished cells. TIMP-1 is an endogenous inhibitor of MMPs, and precisely modulates the proteolytic activities (Gomis-Ruth et al., 1997).

circRNAs have subsequently been revealed to possess miRNAs sponging properties (Rong et al., 2017). Importantly, it has attracted much attention that circRNAs are included in the development of osteosarcoma through functioning as a sponge of miRNAs (Song & Li, 2018; Xu et al., 2018; H. Zhang et al., 2017; X. Zhou et al., 2018). Zhong et al. (2016) showed that through sequestering miR-103a-3p/miR-107 circTCF25 regulates gene expression, suggesting a potential value for therapy and diagnosis. Up-to-now, limited knowledge has been gained on the modulatory role of circTCF25/miR-206. In the current study, we observed a downregulation of miR-206 in circTCF25-overexpressed cells. Recent evidence showed that circRNA containing tandem anti-miRNA sequences attracts, binds and continually quenches natural miRNAs, which ultimately leads to the dysregulation of mRNA targeted by miRNAs (Zhao, Alexandrov, Jaber, & Lukiw, 2016). Therefore, it is a momentous modulatory axis, circRNA–miRNA–mRNA, for pathological processes.

As we presented, miR-206 buffered the oncogenic properties of circTCF25 by abating proliferation, blockading cell cycle, and retarding migration and invasion. Of particular note was that miR-206 offset the carcinogenesis of circTCF25 through downregulating cyclin D1, CDK6, MMPs, and vimentin, and upregulating TIMP-1. The molecular underpinnings might be associated with the target relationship between miRNAs and mRNAs. Cyclin D1 has been ascertained to be a major target of miR-206 (Alteri et al., 2013). Actually, miR-206 has been found to target several mRNAs coding for actin-binding protein coronin 1C (Wang et al., 2014) and sry-related high mobility group box 9 (Y. J. Zhang et al., 2015) involved in the mediation of migration and invasion. As a whole, circTCF25 might induce protein expression involved in proliferation and migration and invasion through repressing miR-206 which induces or governs the accumulation of mRNAs coding for these specific proteins.

Besides direct target regulation, miR-206 has been found to mediate the cancer process via regulating signaling transduction of several pathways (Q. Y. Chen et al., 2016; Pan et al., 2018; X. W. Wang et al., 2015). Here, we dissected whether miR-206 downregulated by circTCF25 mediated the activation of MEK/ERK and AKT/mTOR. Both these two signaling cascades have been reported to modulate the expression of CDK6, MMPs, and vimentin (Liu et al., 2018; Sounni et al., 2010; Zhu et al., 2011). As depicted, circTCF25 initiated the signaling transduction of MEK/ERK and AKT/mTOR cascades by triggering the phosphorylation of signal transducers. By contrast, miR-206 overexpression counteracted the effects of circTCF25. Hence, we concluded that circTCF25 might induce the signaling transduction of MEK/ERK and AKT/mTOR pathways through repressing miR-206 expression.

In summary, the cancerogenic roles played by circTCF25 could be partially modulated via its suppressive effects on a miR-206 expression which buffers cancer process through directly target mRNA or blocking signaling transduction implicated in proliferation as well as migration and invasion of osteosarcoma cells.

CONFLICT OF INTERESTS

The authors declare that there are no conflict of interests.

AUTHOR CONTRIBUTIONS

Y. W., S. S., and J. Z. conceived and designed the experiments; Y. W., S. S., and Q. Z. performed the experiments and analyzed the data; Q. Z. and H. D. contributed reagents/materials/analysis tools; Y. W. and J. Z. wrote the manuscript.

DATA AVAILABILITY STATEMENT

The datasets used and/or analyzed during the current study are available from the corresponding author on reasonable request.

ETHICS STATEMENT

All procedures performed in studies involving human participants were in accordance with the ethical standards of the institutional committee and with the 1964 Helsinki declaration and its later amendments or comparable ethical standards. Every patient agreed with joining the research and writing informed consent, and the present research was ratified by the Medical Ethics Committee of China-Japan Union Hospital of Jilin University.

ORCID

Jingzhe Zhang http://orcid.org/0000-0003-2516-5234

REFERENCES

Ali, A., Hu, L., Qian, A., Chen, C., & Yang, T. (2018). Long noncoding RNAs and human osteosarcoma. *Journal of Stem Cell Research Therapy*, *8*(418), 2.

Alteri, A., De Vito, F., Messina, G., Pompili, M., Calconi, A., Visca, P., & Grossi, M. (2013). Cyclin D1 is a major target of miR-206 in cell differentiation and transformation. *Cell Cycle*, *12*(24), 3781–3790. https://doi.org/10.4161/cc.26674

Bao, Y. P., Yi, Y., Peng, L. L., Fang, J., Liu, K. B., Li, W. Z., & Luo, H. S. (2013). Roles of microRNA-206 in osteosarcoma pathogenesis and progression. *Asian Pacific Journal of Cancer Prevention: APJCP*, *14*(6), 3751–3755. https://doi.org/10.7314/apjcp.2013.14.6.3751

Chen, Q. Y., Jiao, D. M., Wu, Y. Q., Chen, J., Wang, J., Tang, X. L., & Wang, Z. (2016). MiR-206 inhibits HGF-induced epithelial-mesenchymal transition and angiogenesis in non-small cell lung cancer via c-Met/PI3k/Akt/mTOR pathway. *Oncotarget*, *7*(14), 18247–18261. https://doi.org/10.18632/oncotarget.7570

Chen, G., Wang, Q., Yang, Q., Li, Z., Du, Z., Ren, M., & Zhang, G. (2018). Circular RNAs hsa_circ_0032462, hsa_circ_0028173, hsa_circ_0005909 are predicted to promote CADM1 expression by functioning as miRNAs sponge in human osteosarcoma. *PLOS One*, *13*(8), e0202896–e0202913. https://doi.org/10.1371/journal.pone.0202896

Dehghannasiri, R., Szabo, L., & Salzman, J. (2019). Ambiguous splice sites distinguish circRNA and linear splicing in the human genome. *Bioinformatics*, *35*(8), 1263–1268. https://doi.org/10.1093/bioinformatics/bty785

Du, W. W., Yang, W., Liu, E., Yang, Z., Dhaliwal, P., & Yang, B. B. (2016). Foxo3 circular RNA retards cell cycle progression via forming ternary complexes with p21 and CDK2. *Nucleic Acids Research*, *44*(6), 2846–2858. https://doi.org/10.1093/nar/gkw027

Elliman, S. J., Howley, B. V., Mehta, D. S., Fearnhead, H. O., Kemp, D. M., & Barkley, L. R. (2014). Selective repression of the oncogene cyclin D1 by the tumor suppressor miR-206 in cancers. *Oncogenesis*, *3*, e113. https://doi.org/10.1038/oncsis.2014.26

Gomis-Ruth, F. X., Maskos, K., Betz, M., Bergner, A., Huber, R., Suzuki, K., & Bode, W. (1997). Mechanism of inhibition of the human matrix metalloproteinase stromelysin-1 by TIMP-1. *Nature*, *389*(6646), 77–81. https://doi.org/10.1038/37995

Isakoff, M. S., Bielack, S. S., Meltzer, P., & Gorlick, R. (2015). Osteosarcoma: Current treatment and a collaborative pathway to success. *Journal of Clinical Oncology*, *33*(27), 3029–3035. https://doi.org/10.1200/jco.2014.59.4895

Li, H. M., Dai, Y. W., Yu, J. Y., Duan, P., Ma, X. L., Dong, W. W., & Li, H. G. (2019). Comprehensive circRNA/miRNA/mRNA analysis reveals circRNAs protect against toxicity induced by BPA in GC-2 cells. *Epigenomics*, *11*(8), 935–949. https://doi.org/10.2217/epi-2018-0217

Liu, J., Duan, Z., Guo, W., Zeng, L., Wu, Y., Chen, Y., & Shi, J. (2018). Targeting the BRD4/FOXO3a/CDK6 axis sensitizes AKT inhibition in luminal breast cancer. *Nature Communications*, *9*(1), 5200. https://doi.org/10.1038/s41467-018-07258-y

Luo, Y. H., Zhu, X. Z., Huang, K. W., Zhang, Q., Fan, Y. X., Yan, P. W., & Wen, J. (2017). Emerging roles of circular RNA hsa_circ_0000064 in the proliferation and metastasis of lung cancer. *Biomedicine & pharmacotherapy = Biomédecine & pharmacothérapie*, *96*, 892–898. https://doi.org/10.1016/j.biopha.2017.12.015

Misaghi, A., Goldin, A., Awad, M., & Kulidjian, A. A. (2018). Osteosarcoma: A comprehensive review. *SICOT-J*, *4*, 12. https://doi.org/10.1051/sicotj/2017028

Palmini, G., Marini, F., & Brandi, M. L. (2017). What is new in the miRNA world regarding osteosarcoma and chondrosarcoma? *Molecules*, *22*(3), 417. https://doi.org/10.3390/molecules22030417

Pan, B. L., Tong, Z. W., Wu, L., Pan, L., Li, J. E., Huang, Y. G., & Li, X. D. (2018). Effects of microRNA-206 on osteosarcoma cell proliferation, apoptosis, migration and invasion by targeting ANXA2 through the AKT signaling pathway. *Cellular Physiology and Biochemistry*, *45*(4), 1410–1422. https://doi.org/10.1159/000487567

Rong, D., Sun, H., Li, Z., Liu, S., Dong, C., Fu, K., & Cao, H. (2017). An emerging function of circRNA-miRNAs-mRNA axis in human diseases. *Oncotarget*, *8*(42), 73271–73281. https://doi.org/10.18632/oncotarget.19154

Smeland, S., Bielack, S. S., Whelan, J., Bernstein, M., Hogendoorn, P., Krailo, M. D., & Marina, N. (2019). Survival and prognosis with osteosarcoma: Outcomes in more than 2000 patients in the EURAMOS-1 (European and American Osteosarcoma Study) cohort. *European Journal of Cancer*, *109*, 36–50. https://doi.org/10.1016/j.ejca.2018.11.027

Song, Y. Z., & Li, J. F. (2018). Circular RNA hsa_circ_0001564 regulates osteosarcoma proliferation and apoptosis by acting miRNA sponge. *Biochemical and Biophysical Research Communications*, *495*(3), 2369–2375. https://doi.org/10.1016/j.bbrc.2017.12.050

Sounni, N. E., Rozanov, D. V., Remacle, A. G., Golubkov, V. S., Noel, A., & Strongin, A. Y. (2010). Timp-2 binding with cellular MT1-MMP stimulates invasion-promoting MEK/ERK signaling in cancer cells. *International Journal of Cancer*, *126*(5), 1067–1078. https://doi.org/10.1002/ijc.24690

Wang, J., & Li, H. (2018). CircRNA circ_0067934 silencing inhibits the proliferation, migration and invasion of NSCLC cells and correlates with unfavorable prognosis in NSCLC. *European Review for Medical and Pharmacological Sciences*, *22*(10), 3053–3060. https://doi.org/10.26355/eurrev_201805_15063

Wang, C., Ren, M., Zhao, X., Wang, A., & Wang, J. (2018). Emerging roles of circular RNAs in osteosarcoma. *Medical Science Monitor*, *24*, 7043–7050. https://doi.org/10.12659/msm.912092

Wang, J., Tsouko, E., Jonsson, P., Bergh, J., Hartman, J., Aydogdu, E., & Williams, C. (2014). miR-206 inhibits cell migration through direct targeting of the actin-binding protein coronin 1C in triple-negative breast cancer. *Molecular Oncology*, *8*(8), 1690–1702. https://doi.org/10.1016/j.molonc.2014.07.006

Wang, X. W., Xi, X. Q., Wu, J., Wan, Y. Y., Hui, H. X., & Cao, X. F. (2015). MicroRNA-206 attenuates tumor proliferation and migration involving the downregulation of NOTCH3 in colorectal cancer. *Oncology Reports*, *33*(3), 1402–1410. https://doi.org/10.3892/or.2015.3731

Wang, S. H., Zhang, W. J., Wu, X. C., Zhang, M. D., Weng, M. Z., Zhou, D., & Quan, Z. W. (2016). Long non-coding RNA Malat1 promotes gallbladder cancer development by acting as a molecular sponge to regulate miR-206. *Oncotarget*, *7*(25), 37857–37867. https://doi.org/10.18632/oncotarget.9347

Xi, Y., Fowdur, M., Liu, Y., Wu, H., He, M., & Zhao, J. (2019). Differential expression and bioinformatics analysis of circRNA in osteosarcoma. *Bioscience Reports*, *39*(5), BSR20181514–BSR20181524. https://doi.org/10.1042/bsr20181514

Xu, B., Yang, T., Wang, Z., Zhang, Y., Liu, S., & Shen, M. (2018). CircRNA CDR1as/miR-7 signals promote tumor growth of osteosarcoma with a potential therapeutic and diagnostic value. *Cancer Management and Research*, *10*, 4871–4880. https://doi.org/10.2147/cmar.s178213

Zhang, L., Liu, X., Jin, H., Guo, X., Xia, L., Chen, Z., & Fan, D. (2013). miR-206 inhibits gastric cancer proliferation in part by repressing cyclinD2. *Cancer Letters*, *332*(1), 94–101. https://doi.org/10.1016/j.canlet.2013.01.023

Zhang, H., Wang, G., Ding, C., Liu, P., Wang, R., Ding, W., & Ji, F. (2017). Increased circular RNA UBAP2 acts as a sponge of miR-143 to promote osteosarcoma progression. *Oncotarget*, *8*(37), 61687–61697. https://doi.org/10.18632/oncotarget.18671

Zhang, Y. J., Xu, F., Zhang, Y. J., Li, H. B., Han, J. C., & Li, L. (2015). miR-206 inhibits non small cell lung cancer cell proliferation and invasion by targeting SOX9. *International Journal of Clinical and Experimental Medicine*, *8*(6), 9107–9113.

Zhao, Y., Alexandrov, P. N., Jaber, V., & Lukiw, W. J. (2016). Deficiency in the ubiquitin conjugating enzyme UBE2A in Alzheimer's disease (AD) is linked to deficits in a natural circular miRNA-7 sponge (circRNA; ciRS-7). *Genes (Basel)*, *7*(12), 116. https://doi.org/10.3390/genes7120116.

Zhong, Z., Lv, M., & Chen, J. (2016). Screening differential circular RNA expression profiles reveals the regulatory role of circTCF25-miR-103a-3p/miR-107-CDK6 pathway in bladder carcinoma. *Scientific Reports*, *6*, 30919. https://doi.org/10.1038/srep30919

Zhou, X., Natino, D., Qin, Z., Wang, D., Tian, Z., Cai, X., & He, X. (2018). Identification and functional characterization of circRNA-0008717 as an oncogene in osteosarcoma through sponging miR-203. *Oncotarget*, *9*(32), 22288–22300. https://doi.org/10.18632/oncotarget.23466

Zhou, J., Tian, Y., Li, J., Lu, B., Sun, M., Zou, Y., & Ji, G. (2013). miR-206 is down-regulated in breast cancer and inhibits cell proliferation through the up-regulation of cyclinD2. *Biochemical and Biophysical Research Communications*, *433*(2), 207–212. https://doi.org/10.1016/j.bbrc.2013.02.084

Zhu, Q. S., Rosenblatt, K., Huang, K. L., Lahat, G., Brobey, R., Bolshakov, S., & Lev, D. (2011). Vimentin is a novel AKT1 target mediating motility and invasion. *Oncogene*, *30*(4), 457–470. https://doi.org/10.1038/onc.2010.421

How to cite this article: Wang Y, Shi S, Zhang Q, Dong H, Zhang J. MicroRNA-206 upregulation relieves circTCF25-induced osteosarcoma cell proliferation and migration. *J Cell Physiol*. 2020;1–10. https://doi.org/10.1002/jcp.29570